

The Nucho-dorsal Glands of *Rhabdophis guangdongensis* (Squamata: Colubridae: Natricinae), with Notes on Morphological Variation and Phylogeny Based on Additional Specimens

Authors: Zhu, Guang-Xiang, Yang, Shijun, Savitzky, Alan H., Zhang, Liang, Cheng, Yuqi, et al.

Source: Current Herpetology, 39(2) : 108-119

Published By: The Herpetological Society of Japan

URL: <https://doi.org/10.5358/hsj.39.108>

BioOne Complete (complete.BioOne.org) is a full-text database of 200 subscribed and open-access titles in the biological, ecological, and environmental sciences published by nonprofit societies, associations, museums, institutions, and presses.

Your use of this PDF, the BioOne Complete website, and all posted and associated content indicates your acceptance of BioOne's Terms of Use, available at www.bioone.org/terms-of-use.

Usage of BioOne Complete content is strictly limited to personal, educational, and non - commercial use. Commercial inquiries or rights and permissions requests should be directed to the individual publisher as copyright holder.

BioOne sees sustainable scholarly publishing as an inherently collaborative enterprise connecting authors, nonprofit publishers, academic institutions, research libraries, and research funders in the common goal of maximizing access to critical research.

The Nucho-dorsal Glands of *Rhabdophis guangdongensis* (Squamata: Colubridae: Natricinae), with Notes on Morphological Variation and Phylogeny Based on Additional Specimens

GUANG-XIANG ZHU^{1,2,*,#}, SHIJUN YANG^{1,#}, ALAN H. SAVITZKY³,
LIANG ZHANG⁴, YUQI CHENG¹, AND JIAJUN WANG¹

¹College of Life Science, Sichuan Agricultural University, Ya'an, Sichuan 625014, China

²Farm Animal Genetic Resources Exploration and Innovation Key Laboratory of Sichuan Province, Sichuan Agricultural University, Chengdu 611130, China

³Department of Biology, Utah State University, Logan, Utah 84322–5305, USA

⁴Guangdong Key Laboratory of Animal Conservation and Resource Utilization, Guangdong Public Laboratory of Wild Animal Conservation and Utilization, Guangdong Institute of Applied Biological Resources, Guangdong 510260, China

Abstract: We report the presence of nucho-dorsal glands in *Rhabdophis guangdongensis*. This recently described species is the 18th member of the genus known to possess integumentary defensive glands. Nine to ten pairs of nuchal glands, separated by a diastema from 116–118 pairs of dorsal glands were observed in two specimens. Because the species was previously known only from the female holotype, we also report data on the size and scalation of five additional specimens and on the morphology of the hemipenis.

Key words: Hemipenis; Morphology; Natricinae

INTRODUCTION

Rhabdophis guangdongensis was first described by Zhu et al. (2014) based on a female specimen (filed No. SYS r000018) from Aizhai Village, Renhua County, Guangdong Province, China. The new species was established on the basis of color pattern, scalation, and molecular distinctiveness.

However, only a single specimen was available at the time of the description.

Nuchal glands were first described in *R. tigrinus* (Nakamura, 1935). The organs are embedded in the dermis of the neck region as a series of paired glands and are considered to have defensive function that is reflected in their unique chemical and behavioral features (Mori et al., 2012). Nuchal glands and the homologous nucho-dorsal glands (which extend the full length of the body; Smith, 1938) have been found in 17 species of *Rhabdophis* (which now includes the nominal genera *Balanophis* and *Macropisthodon*) (Mori et al., 2012, 2016a, b, c; Takeuchi et al.,

*Corresponding author.

E-mail address: ZhuGX0711@163.com

#These authors have contributed equally to this work.

2018). *Rhabdophis guangdongensis* is a member of this monophyletic group, but it was not known whether it possesses nuchal or nucho-dorsal glands.

Here we report data from five additional specimens that confirm the validity of *R. guangdongensis* as a member of the “nuchal gland clade” described by Takeuchi et al. (2018). Moreover, we dissected two specimens of *R. guangdongensis* to determine whether this species possesses nuchal or nucho-dorsal glands. Finally, we present supplementary data on the size and scalation of this species, as well as the first description of the hemipenis.

MATERIALS AND METHODS

Sampling

This study is based on five specimens of *R. guangdongensis* collected in Wutongshan, Shenzhen, Guangdong Province (SICAU 20160801-91 and SICAU201509013-305), Nankunshan, Huizhou, Guangdong Province (ZL-RG-2018-0421; Fig. 1A), Yinpingshan, Dongguan, Guangdong Province (ZL-RG-2014-4-10; Fig. 1B), and Tianjingshan, Shaoguan, Guangdong Province (ZL-RG-2017-0423; Fig. 1C). The sample number shows the exact date of collection. Skin glands were examined in two of those specimens (SICAU201509013-305 and ZL-RG-2017-0423). The hemipenes were examined in one specimen (SICAU20160801-91). Identification of these five individuals was based on the description by Zhu et al. (2014) and confirmed by our molecular analysis. Fresh liver tissue was collected from all specimens and immediately preserved in 95% ethanol. The specimens were then fixed in 10% buffered formalin and later transferred to 70% ethanol.

Phylogenetic analyses

The phylogeny was generated from the concatenated sequences of cytochrome b (cyt b) and c-mos. Sequences are aligned by Mega 5.0 (Tamura et al., 2011). We analyzed 37 sequences from species in the genus *Rhabdo-*

phis, and used *Pseudagkistrodon rudis* (three sequences) and *Hebius atemporale* (one sequence) as outgroups. The sequences used for constructing a phylogenetic tree are shown in Appendix I. We analyzed the molecular data using both Bayesian inference (BI) and maximum likelihood (ML). The best-fitting model of sequence evolution for BI was obtained using PartitionFinder 2.1.1 (Lanfear et al., 2017), according to the Bayesian information criterion (Schwarz, 1978), using MrBayes 3.1.2 (Huelsenbeck and Ronquist, 2001). For the BI analysis, posterior distributions were obtained by Markov Chain Monte Carlo (MCMC) analysis, with four chains for 10 million generations and sampled every 100th generation. The first 25% of the trees were discarded (burn-in). Maximum likelihood analyses were performed with RAxML 8.2.10 (Stamatakis, 2014) under the GTRGAMMA model and included 1000 bootstrap replicates.

Examination of morphology, integumentary glands, and hemipenes

We peeled the skin to expose the skin glands as described by Mori et al. (2016a). The length and width of the first five, last five and every 25th intervening glands were measured as in Mori et al. (2016a). Moreover, we calculated the area of the gland as length×width; length was measured parallel to the longitudinal body axis, and width was measured along the transverse axis. The position of the glands in relation to dorsal scale rows was recorded as follows: the middorsal scale row, along the vertebral line, was defined as row zero, and the number of scale rows was counted in the ventrolateral direction on each side until reaching the scale under which the glands were positioned.

The following morphological characters were measured with a ruler to the nearest millimeter: snout-vent length (SVL) and tail length (TaL). The following scale counts were recorded: number of supraoculars (SPO), preoculars (PRO), postoculars (PTO), loreals (LR), temporals (TEM), supralabials (SL),



FIG. 1. Photos of *Rhabdophis guangdongensis*. A: ZL-RG-2018-0421; B: ZL-RG-2014-4-10; C: ZL-RG-2017-0423. Photos by Liang Zhang.

infralabials (IL), ventrals (VEN), dorsal scale rows (DSR), and subcaudals (SC). Character definitions and counting methods followed Zhao (2006). Identification of sex was performed by dissection. The method of everting and fixing the hemipenis followed Jiang (2010), and hemipenial morphology follows Dowling and Savage (1960) and Zhang et al. (1984).

RESULTS

Phylogenetic analysis

The topological structure of the ML and BI trees are nearly identical (data not shown). The five recently collected specimens reported in this study are grouped with the holotype of *R. guangdongensis* (SYS r000018), with high support (Fig. 2). These phylogenetic results, combined with the distinctive coloration and

morphological characteristics of these specimens, are consistent with the original description of *R. guangdongensis* (Zhu et al., 2014; see below), confirming the identity of these new specimens.

Morphological supplementary descriptions of Rhabdophis guangdongensis

The coloration of the new specimens in life closely resembled that of the holotype (Fig. 1; also see figures of Zhu et al., 2014). Following preservation in ethanol, the colors faded from grey-brown to gray and from orange to yellowish-white.

The scalation and measurements of the five new specimens is shown in Table 1 and are compared with values for the holotype. All six of those specimens share these characteristics: DSR 15 throughout; dorsal scales feebly keeled except the outermost rows, which are

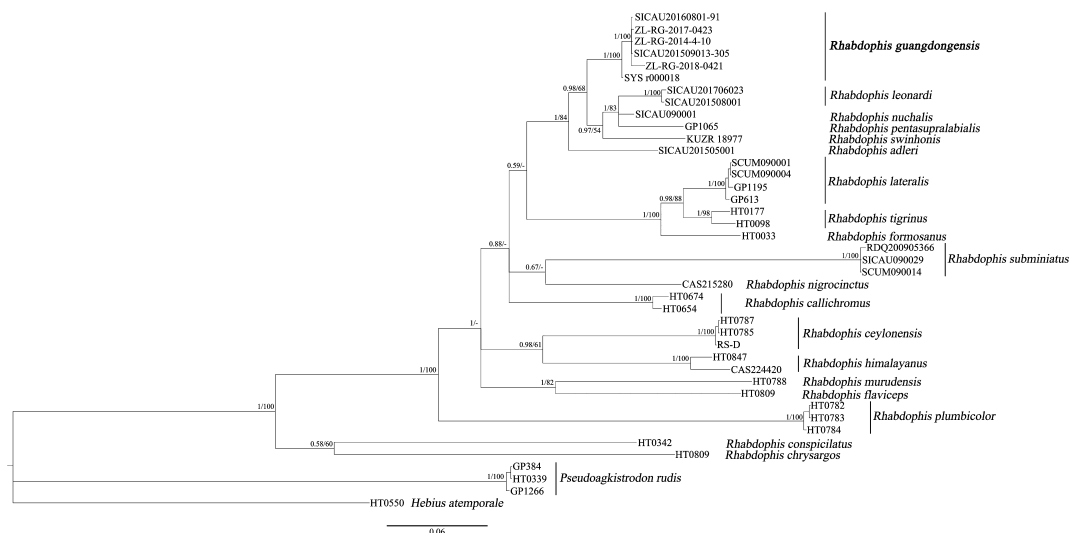


FIG. 2. Bayesian inference and maximum likelihood phylogenetic tree based on concatenated cytochrome b and c-mos gene sequences. The phylogenetic tree shown is based on the Bayesian tree topology, adding the posterior probability (PP) and bootstrap (BS) values of the nodes (PP/BS). Hyphen (-) represents <50 BS support.

smooth; SPO, PRO, and LR single; SL six. However, PTO vary from 2–3 and IL vary from 7–8 in the new specimens. The maxillary dentition is similar to that of other *Rhabdophis* species, with the last two teeth enlarged.

SICAU20160801-91 is the only male specimen and has the shortest SVL (341 mm) and the longest TaL (94 mm) of any other specimen. This result is consistent with the longer tail of males in most other snake species. VEN and SC in this male specimen are 123 and 44, respectively. By comparison, the mean VEN and SC of the five known females (including the holotype) are 125.2 and 41.2, respectively.

Nucho-dorsal glands

In each of the two dissected specimens, two longitudinal rows of the nucho-dorsal glands were found. The nucho-dorsal glands occur throughout the entire length of the body (Fig. 3), except for a diastema of approximately 10 body segments between the glands of the neck and body (Fig., 3A1, 3B1). For SICAU 201509013-305, nine pairs of glands were

found in the neck region (the first one on the left is not shown due to an error in peeling the skin, but it was present; see Fig. 3A1). Hereafter, this series of glands is referred to as the nuchal glands. ZL-RG-2017-0423 has 10 pairs of nuchal glands (Fig. 3B1). The nuchal glands start at the posterior margin of the parietals and extend under the dorsal scales to the level of the eighth ventral scale. These nine or ten nuchal glands gradually become larger and are located between the first and second dorsal scale row from the midline.

The trunk series, referred to as the dorsal glands, are noticeably smaller than the nuchal glands (Fig. 3A1). They are essentially symmetrical and total 118 and 116 pairs in SICAU201509013-305 and ZL-RG-2017-0423, respectively. Approximately one pair of dorsal glands is associated with each ventral scale. The dorsal glands are located between the second and third dorsal scale rows from the midline. The dorsal glands tended to be larger in the midbody than in the anterior or posterior trunk (Fig. 4, Appendix II).

TABLE 1. The pholidosis characteristics and some measurable data of five specimens of *Rhabdophis guangdongensis*. See text for abbreviations.

| Voucher specimen | Sex | SVL (mm) | TaL (mm) | VEN | DSR | SC | SPO | PRO | PTO (left/right) | LR | TEM (left/right) | SL | IL (left/right) |
|-----------------------|--------|----------|----------|-----|----------|----|-----|-----|------------------|----|------------------|----|-----------------|
| SYS r00018 (Holotype) | Female | 449 | 88 | 126 | 15-15-15 | 39 | 1 | 1 | 2/2 | 1 | 1+1/1+1 | 6 | 7/7 |
| SICAU20160801-91 | Male | 341 | 94 | 123 | 15-15-15 | 44 | 1 | 1 | 3/3 | 1 | 1+1/1+1 | 6 | 8/8 |
| SICAU201509013-305 | Female | 426 | 90 | 127 | 15-15-15 | 38 | 1 | 1 | 2/3 | 1 | 1+1/1+1 | 6 | 8/8 |
| ZL-RG-2017-0423 | Female | 377 | 84 | 126 | 15-15-15 | 42 | 1 | 1 | 3/3 | 1 | 1+1/1+1 | 6 | 8/7 |
| ZL-RG-2018-0421 | Female | 285 | 71 | 122 | 15-15-15 | 47 | 1 | 1 | 3/3 | 1 | 1+1/1+2 | 6 | 8/8 |
| ZL-RG-2014-4-10 | Female | 475 | 84 | 125 | 15-15-15 | 40 | 1 | 1 | 3/2 | 1 | 1+1/1+1 | 6 | 8/8 |

Hemipenes

The retracted hemipenis extends to the twelfth subcaudal, and the fork is at the level of the tenth subcaudal. The everted hemipenis is bilobed (Fig. 5). The organ measures 17.16 mm and the lobes measure 2.05 mm (12% of hemipenial length). The entire everted hemipenis bears spines, which gradually increase in size toward the base of the organ. There is a large basal spine located opposite to the base of the sulcus spermaticus. The sulcus extends up the center of the base and along the proximal three-quarters each lobe. The edges of the sulcus are smooth.

DISCUSSION

This report of nucho-dorsal glands in *R. guangdongensis* raises the number of species that possess nuchal glands or nucho-dorsal glands to 18. *Rhabdophis guangdongensis* was the only species included in the molecular phylogeny of Takeuchi et al. (2018) for which the condition of the nuchal glands was not known (Other six species of *Rhabdophis* lacked both information on their defensive glands and sequence data, and thus were not included in that phylogenetic analysis or ours). Our phylogenetic tree is similar in a number of respects to that of Takeuchi et al. (2018), although there are also several important differences. The similarities include a monophyletic “nuchal gland clade” (NGC; *sensu* Takeuchi et al., 2018), which includes all those species of Asian natricines for which either nuchal or nucho-dorsal glands are known, as well as three species for which data on the presence of the glands is either ambiguous or reflects intraspecific variation. As in the phylogeny of Takeuchi et al. (2018), our analysis places *R. conspicillatus* and *R. chrysargos* outside the NGC, and we recover *R. plumbicolor* as the most basal member of the NGC. Our analysis also finds that *R. flaviceps* and *R. murudensis* form a sister-species pair, as do *R. ceylonicus* and *R. himalayanus*. These results support the synonymy of *Macropisthodon* (formerly including *R.*

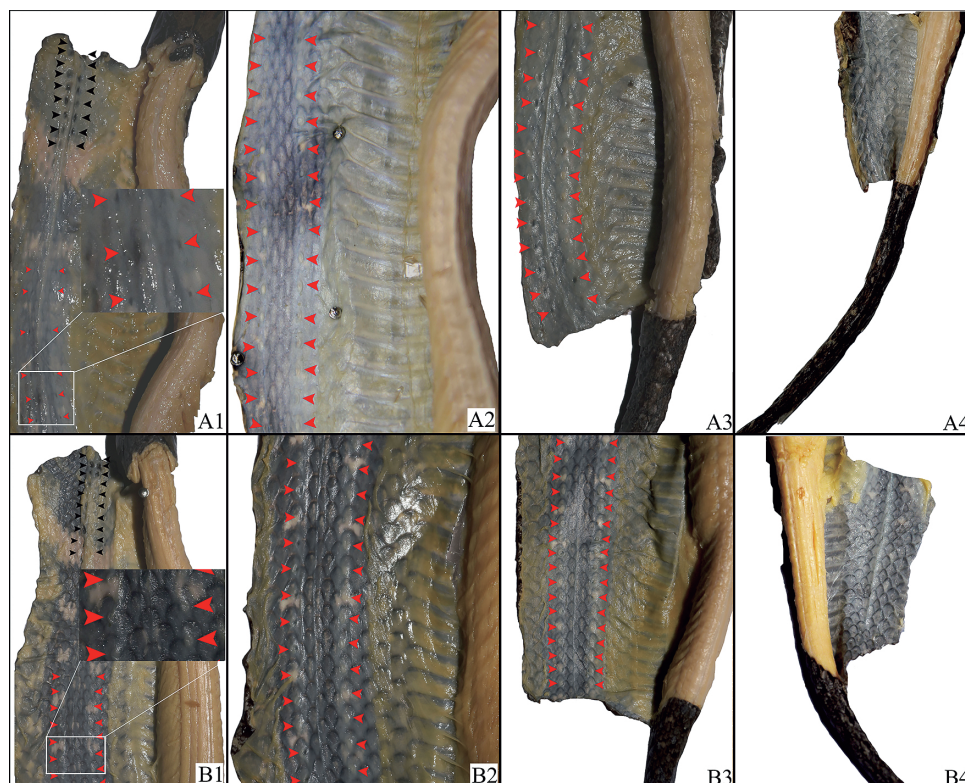


FIG. 3. Nucho-dorsal glands of *Rhabdophis guangdongensis* (A: SICAU201509013-305; B: ZL-RG-2017-0423). (1) The glands in the neck and anterior part of the body; (2) in the middle part of the body; (3) in the posterior part of the body. Black arrowhead indicates nuchal gland, red arrowhead represents dorsal gland; (4) no gland on the tail. Photo by Yuqi Cheng and Guang-Xiang Zhu.

plumbicolor and *R. flaviceps*) and *Balano-*
phis (formerly including *R. ceylonicus*) in
Rhabdophis, as proposed by Takeuchi et al.
(2018). Our results also support the monophyly of the three species of the *R. tigrinus* group, with *R. formosanus* sister to *R. tigrinus*+*R. lateralis* (Takeuchi et al., 2011, 2014, 2018). Finally, we agree with Takeuchi et al. (2018) in recovering a derived clade that includes *R. nuchalis*, *R. pentasupralabialis*, and *R. leonardi*, known as the *R. nuchalis* group (Yoshida et al., 2020). Furthermore, both Takeuchi et al. (2018) and we find that *R. guangdongensis* and *R. swinhonis* are more closely related to the *R. nuchalis* group than to other *Rhabdophis*. However, our analysis places *R. swinhonis* closer to that

group than is *R. guangdongensis*, whereas Takeuchi et al. (2018) consider *R. guangdongensis* closer to the *R. nuchalis* group than is *R. swinhonis*. Importantly, all three species of the *R. nuchalis* group possess nucho-dorsal, rather than nuchal, glands, as does *R. guangdongensis* (Mori et al., 2012). The condition of the nuchal glands in *R. swinhonis* is uncertain and may vary intraspecifically (Takeuchi et al., 2018).

In addition to the relative order of *R. guangdongensis* and *R. swinhonis* as successive sister taxa to the *R. nuchalis* group, there are several other differences between the phylogeny of Takeuchi et al. (2018) and ours. Those authors recognize *R. adleri* as sister to *R. callichromis*, and those two as sister to *R.*

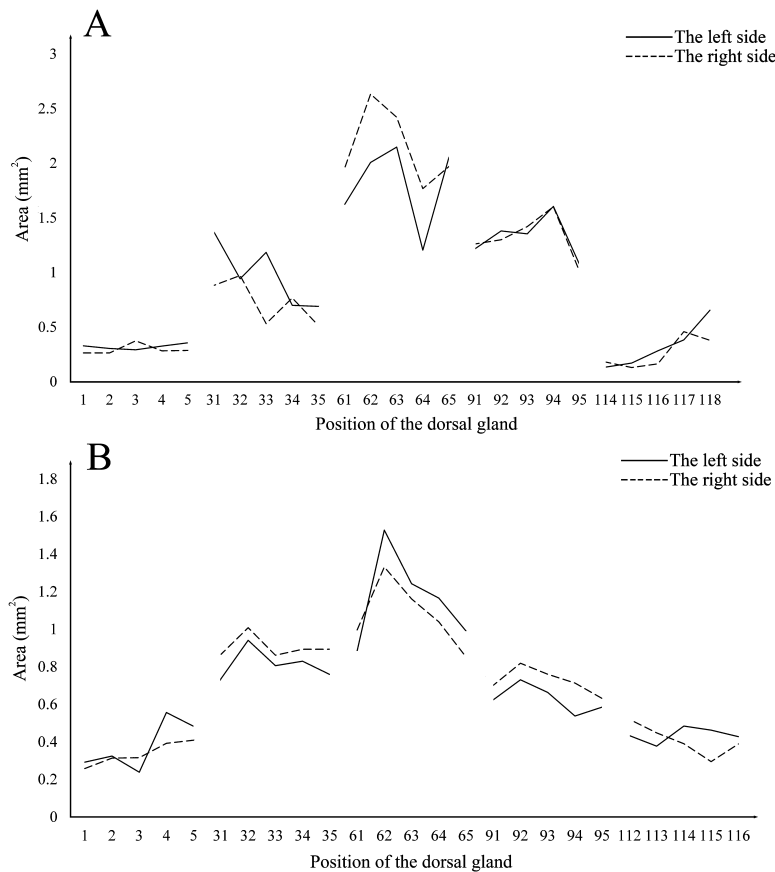


FIG. 4. Sizes of the dorsal glands (A: SICAU201509013-305; B: ZL-RG-2017-0423). The nuchal series of glands is not included. See Appendix II for measurements.

nigrocinctus. Our phylogeny, in contrast, places *R. adleri* as sister to *R. guangdongensis*+*R. swinhonis*+*R. nuchalis* group. We recover *R. nigrocinctus* as sister to *R. subminiatus*, and the position of *R. callichromis* is not fully resolved in our phylogeny. Furthermore, Takeuchi et al. (2018) placed *R. subminiatus* considerably closer to the base of the NGC than does our phylogeny. Of the 41 molecular samples included in our analysis, 19 (46%; Appendix I) are not represented in the phylogeny of Takeuchi et al. (2018). Taken together, these results suggest a reasonable level of agreement on the phylogeny of this genus, although a number of taxa remain to be placed with confidence on the tree.

Takeuchi et al. (2018) found evidence of substantial variation within several nominal species, so it is possible that differences in population sampling could explain some of the inconsistencies between our trees.

The pattern of variation in the size of dorsal glands along the trunk in *R. guangdongensis* is similar to that observed in *R. nuchalis*, *R. pentasupralabialis*, and *R. adleri*, with the largest glands occurring in the middle part of the trunk (Mori et al., 2016a, c). Moreover, *R. guangdongensis*, along with *R. nuchalis* and *R. pentasupralabialis*, possesses a diastema between the nuchal and dorsal glands (Mori et al., 2016c). However, arrangement of nucho-dorsal glands is highly variable

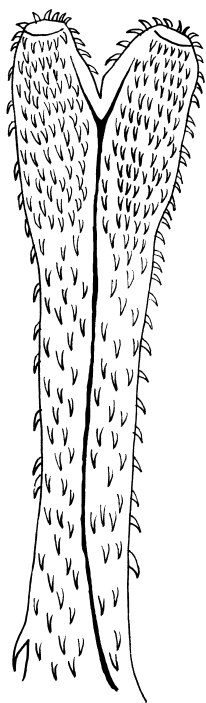


FIG. 5. The hemipenis of *Rhabdophis guangdongensis* (SICAU20160801-91). Drawing by Shijun Yang.

among species, and the number of glands and the length of the diastema also vary inter- and intraspecifically (Smith, 1938; Mori et al., 2016c). It is not yet known whether this variation reflects differences between populations or only between individuals (Mori et al., 2016c).

This is the first description of the hemipenis of *R. guangdongensis*, and the organ is similar to that of most other *Rhabdophis*, such as *R. nuchalis*, *R. adleri*, and *R. leonardi* (Zhu et al., 2013).

ACKNOWLEDGMENTS

This study was supported in part by a grant of the National Natural Science Foundation of China (NSFC31401959) and a grant from the China Postdoctoral Foundation (2016M592688). Additional support was also provided by the China Scholarship Council

(Grant no. CSC201706915015) and the Postdoctoral Foundation of the Sichuan Provincial Human Resources and Social Security Department to Zhu GX. This research was also supported in part by project grant GDAS Special Project of Science and Technology Development (2017GDASCX-0107). We acknowledge Wenjiao Tang for her help with collection of the morphological data. We are grateful to Hannah Wilson (Utah State University) for her kind editorial assistance and professional advice.

LITERATURE CITED

- DOWLING, H. G. AND SAVAGE, J. M. 1960. A guide to the snake hemipenis: A survey of basic structure and systematic characteristics. *Zoologica New York* 45: 17–28.
- GUO, P., LIU, Q., XU, Y., JIANG, K., HOU, M., DING, L., PYRON, R. A., AND BURBRINK, F. T. 2012. Out of Asia: Natricine snakes support the Cenozoic Beringian dispersal hypothesis. *Molecular Phylogenetics and Evolution* 63: 825–833.
- GUO, P., ZHU, F., LIU, Q., ZHANG, L., LI, J.-X., HUANG, Y.-Y., AND PYRON, R. A. 2014. A taxonomic revision of the Asian keelback snakes, genus *Amphiesma* (Serpentes: Colubridae: Natricinae), with description of a new species. *Zootaxa* 3873: 425–440.
- HUELSENBECK, J. P. AND RONQUIST, F. 2001. MRBAYES: Bayesian inference of phylogenetic trees. *Bioinformatics* 17: 754–755.
- JIANG, K. 2010. A method for evaginating the hemipenis of preserved snakes. *Sichuan Journal of Zoology* 29: 122–123.
- LANFEAR, R., FRANSEN, P. B., WRIGHT, A. M., SENFELD, T., AND CALCOTT, B. 2017. Partition-Finder 2: New methods for selecting partitioned models of evolution for molecular and morphological phylogenetic analyses. *Molecular Biology and Evolution* 34: 772–773.
- MORI, A., BURGHARDT, G. M., SAVITZKY, A. H., ROBERTS, K. A., HUTCHINSON, D. A., AND GORIS, R. C. 2012. Nuchal glands: A novel defensive system in snakes. *Chemoecology* 22: 187–198.

- MORI, A., JONO, T., DING, L., ZHU, G.-X., WANG, J., SHI, H.-T., AND TANG, Y. 2016a. Discovery of nucho-dorsal glands in *Rhabdophis adleri*. *Current Herpetology* 35: 53–58.
- MORI, A., JONO, T., TAKEUCHI, H., AND DAS, I. 2016b. *Rhabdophis conspicillatus* (Red-bellied Keelback), Morphology. *Herpetological Review* 47: 482–483.
- MORI, A., JONO, T., TAKEUCHI, H., DING, L., DE SILVA, A., MAHAULPATHA, D., AND TANG, Y. 2016c. Morphology of the nucho-dorsal glands and related defensive displays in three species of Asian natricine snakes. *Journal of Zoology* 300: 18–26.
- NAKAMURA, K. 1935. On a new integumental poison gland found in the nuchal region of a snake, *Natrix tigrina*. *Memoirs of the College of Science, Kyoto Imperial University, Series B* 10: 229–240, 1 pl.
- PYRON, R. A., KANDAMDI, H. K. D., HENDRY, C. R., PUSHPAMAL, V., BURBRINK, F. T., AND SOMAWEERA, R. 2013. Genus-level phylogeny of snakes reveals the origins of species richness in Sri Lanka. *Molecular Phylogenetics and Evolution* 66: 969–978.
- SCHWARZ, G. 1978. Estimating the dimension of a model. *Annals of Statistics* 6: 461–464.
- SMITH, M. A. 1938. The nucho-dorsal glands of snakes. *Proceedings of the Zoological Society of London, Series B* 100: 575–583.
- STAMATAKIS, A. 2014. RAxML version 8: A tool for phylogenetic analysis and post-analysis of large phylogenies. *Bioinformatics* 30: 1312–1313.
- TAKEUCHI, H., SAVITZKY, A. H., DING, L., DE SILVA, A., DAS, I., NGUYEN, T. T., TSAI, T., JONO, T., ZHU, G.-X., MAHAULPATHA, D., TANG, Y., AND MORI, A. 2018. Evolution of nuchal glands, unusual defensive organs of Asian natricine snakes (Serpentes: Colubridae), inferred from a molecular phylogeny. *Ecology and Evolution* 8: 10219–10232.
- TAKEUCHI, H., ZHU, G.-X., DING, L., TANG, Y., OTA, H., MORI, A., OH, H.-S., AND HIKIDA, T. 2014. Taxonomic validity and phylogeography of the East Eurasian natricine snake, *Rhabdophis lateralis* (Berthold, 1859) (Serpentes: Colubridae), as inferred from mitochondrial DNA sequence data. *Current Herpetology* 33: 148–153.
- TAMURA, K., PETERSON, D., PETERSON, N., STECHER, G., NEI, M., AND KUMAR, S. 2011. MEGA5: Molecular evolutionary genetics analysis using maximum likelihood, evolutionary distance, and maximum parsimony methods. *Molecular Biology and Evolution* 28: 2731–2739.
- YOSHIDA, T., UJIE, R., SAVITZKY, A. H., JONO, T., INOUE, T., YOSHINAGA, N., ABURAYA, S., AOKI, W., TAKEUCHI, H., DING, L., CHEN, Q., CAO, C., TSAI, T.-S., DE SILVA, A., MAHAULPATHA, D., NGUYEN, T. T., TANG, Y., MORI, N., AND MORI, A. 2020. Dramatic dietary shift maintains sequestered toxins in chemically defended snakes. *Proceedings of the National Academy of Sciences* 117: 5964–5969.
- ZHANG, F. J., HU, S. Q., AND ZHAO, E. M. 1984. A comparative study on the hemipenial morphology of Colubrinae and its evolutionary relationship in China. *Journal of Amphibians and Reptiles* 3: 23–44.
- ZHAO, E. 2006. *Snakes of China*. Anhui Science and Technology Publishing House, Hefei.
- ZHU, G.-X., GUO, P., AND ZHAO, E. 2013. Comparative studies on hemipenial morphology of eight species of keelback snakes (Serpentes: Colubridae: *Rhabdophis*). *Sichuan Journal of Zoology* 32: 380–384.
- ZHU, G.-X., WANG, Y.-Y., TAKEUCHI, H., AND ZHAO, E. 2014. A new species of the genus *Rhabdophis* Fitzinger, 1843 (Squamata: Colubridae) from Guangdong Province, southern China. *Zootaxa* 3765: 469–480.

Accepted: 11 June 2020

APPENDIX I

Information on all specimens used in the study.

| ID | Current genus and species name | Locality | Voucher specimen | Accession no. of GenBank | | Reference |
|----|----------------------------------|----------------------------|--------------------|--------------------------|----------|----------------------|
| | | | | c-mos | cyt b | |
| 1 | <i>Hebius atemporale</i> | China | HT0550 | LC325766 | LC325320 | Takeuchi et al. 2018 |
| 2 | <i>Pseudogkistirodon rudis</i> | China | HT0339 | LC325757 | LC325311 | Takeuchi et al. 2018 |
| 3 | <i>Pseudogkistirodon rudis</i> | China | GP1266 | JQ687434 | JQ687452 | Guo et al. 2014 |
| 4 | <i>Pseudogkistirodon rudis</i> | China | GP384 | JQ687442 | GQ281780 | Guo et al. 2012 |
| 5 | <i>Rhabdophis adleri</i> | Hainan, China | SICAU201505001 | MK987081 | MK987076 | This study |
| 6 | <i>Rhabdophis callichromus</i> | Vietnam | HT0654 | LC325770 | LC325324 | Takeuchi et al. 2018 |
| 7 | <i>Rhabdophis callichromus</i> | Vietnam | HT0674 | LC325771 | LC325325 | Takeuchi et al. 2018 |
| 8 | <i>Rhabdophis ceylonensis</i> | Sri Lanka | HT0785 | LC325785 | LC325339 | Takeuchi et al. 2018 |
| 9 | <i>Rhabdophis ceylonensis</i> | Sri Lanka | HT0787 | LC325786 | LC325340 | Takeuchi et al. 2018 |
| 10 | <i>Rhabdophis ceylonensis</i> | Sri Lanka | RS-D | KC347384 | KC347474 | Pyron et al. 2013 |
| 11 | <i>Rhabdophis chrysgos</i> | Malaysia | HT0342 | LC325759 | LC325313 | Takeuchi et al. 2018 |
| 12 | <i>Rhabdophis conspiciatulus</i> | Malaysia | HT0791 | LC325788 | LC325342 | Takeuchi et al. 2018 |
| 13 | <i>Rhabdophis flaviceps</i> | Malaysia | HT0809 | LC325801 | LC325355 | Takeuchi et al. 2018 |
| 14 | <i>Rhabdophis formosanus</i> | Taiwan, China | HT0033 | LC325750 | LC325304 | Takeuchi et al. 2018 |
| 15 | <i>Rhabdophis guangdongensis</i> | Shaoguan, Guangdong, China | SYS r000018 | KF800920 | KF800930 | Zhu et al. 2014 |
| 16 | <i>Rhabdophis guangdongensis</i> | Shaoguan, Guangdong, China | SICAU20160801-91 | MN338064 | MN338059 | This study |
| 17 | <i>Rhabdophis guangdongensis</i> | Dongguan, Guangdong, China | ZL-RG-2017-0423 | MN338065 | MN338060 | This study |
| 18 | <i>Rhabdophis guangdongensis</i> | Shenzhen, Guangdong, China | ZL-RG-2014-4-10 | MN338066 | MN338061 | This study |
| 19 | <i>Rhabdophis guangdongensis</i> | Shenzhen, Guangdong, China | SICAU201509013-305 | MN338067 | MN338062 | This study |
| 20 | <i>Rhabdophis guangdongensis</i> | Huizhou, Guangdong, China | ZL-RG-2018-0421 | MN338068 | MN338063 | This study |

APPENDIX I

(continued)

| ID | Current genus and species name | Locality | Voucher specimen | Accession no. of GenBank | | Reference |
|----|---------------------------------------|---------------------------|------------------|--------------------------|----------|----------------------|
| | | | | c-mos | cyt b | |
| 21 | <i>Rhabdophis himalayanus</i> | Kachin State, Myanmar | CAS224420 | KF800919 | KF800929 | Zhu et al. 2014 |
| 22 | <i>Rhabdophis himalayanus</i> | China | HT0847 | LC325746 | LC325299 | Takeuchi et al. 2018 |
| 23 | <i>Rhabdophis lateralis</i> | Tianshui, Gansu, China | SCUM090004 | KF765391 | KF765396 | Zhu et al. 2014 |
| 24 | <i>Rhabdophis lateralis</i> | Huangshan, Anhui, China | GF1195 | KF765390 | KF765395 | Zhu et al. 2014 |
| 25 | <i>Rhabdophis lateralis</i> | Longnan, Gansu, China | SCUM090001 | KF765392 | KF765397 | Zhu et al. 2014 |
| 26 | <i>Rhabdophis lateralis</i> | Liaoning, China | GP613 | Q281785 | JQ687444 | Guo et al. 2014 |
| 27 | <i>Rhabdophis leonardi</i> | Cayu, Xizang, China | SICAU201706023 | MK987082 | MK987075 | This study |
| 28 | <i>Rhabdophis leonardi</i> | Cayu, Xizang, China | SICAU201508001 | MK987081 | MK987074 | This study |
| 29 | <i>Rhabdophis murudensis</i> | Malaysia | HT0788 | LC325787 | LC325341 | Takeuchi et al. 2018 |
| 30 | <i>Rhabdophis nigrocinctus</i> | Shan State, Myanmar | CAS215280 | KF800926 | KF800936 | Zhu et al. 2014 |
| 31 | <i>Rhabdophis nuchalis</i> | Shennongjia, Hubei, China | SICAU090001 | KF800925 | KF800935 | Zhu et al. 2014 |
| 32 | <i>Rhabdophis penitasupralabialis</i> | Jiulong, Sichuan, China | GP1065 | KF800924 | KF800934 | Zhu et al. 2014 |
| 33 | <i>Rhabdophis plumbicolor</i> | Sri Lanka | HT0782 | LC325782 | LC325336 | Takeuchi et al. 2018 |
| 34 | <i>Rhabdophis plumbicolor</i> | Sri Lanka | HT0783 | LC325783 | LC325337 | Takeuchi et al. 2018 |
| 35 | <i>Rhabdophis plumbicolor</i> | Sri Lanka | HT0784 | LC325784 | LC325338 | Takeuchi et al. 2018 |
| 36 | <i>Rhabdophis subminiatus</i> | Baoshan, Yunnan, China | RDQ200905366 | KF765393 | KF765398 | Zhu et al. 2014 |
| 37 | <i>Rhabdophis subminiatus</i> | Panzhihua, Sichuan, China | SCUM090014 | KF765394 | KF800927 | Zhu et al. 2014 |
| 38 | <i>Rhabdophis subminiatus</i> | Hong Kong, China | SICAU090029 | KF800918 | KF800928 | Zhu et al. 2014 |
| 39 | <i>Rhabdophis swinhonis</i> | Taiwan, China | KUZR 18977 | AB861888 | AB842176 | Zhu et al. 2014 |
| 40 | <i>Rhabdophis tigrinus</i> | Japan | HT0098 | LC325751 | LC325305 | Takeuchi et al. 2018 |
| 41 | <i>Rhabdophis tigrinus</i> | Japan | HT0177 | LC325752 | LC325306 | Takeuchi et al. 2018 |

APPENDIX II

The size of the dorsal glands. See text for the measurement method.

| | | SICAU201509013-305 | | | | ZL-RG-2017-0423 | | | |
|------------------------------|-------------|--------------------|-------------|------------|------------------------------|-----------------|------------|-------------|------------|
| Position of the dorsal gland | Left | | Right | | Position of the dorsal gland | Left | | Right | |
| | Length (mm) | Width (mm) | Length (mm) | Width (mm) | | Length (mm) | Width (mm) | Length (mm) | Width (mm) |
| 1 | 0.67 | 0.49 | 0.61 | 0.43 | 1 | 0.71 | 0.41 | 0.66 | 0.39 |
| 2 | 0.62 | 0.49 | 0.64 | 0.41 | 2 | 0.81 | 0.4 | 0.68 | 0.46 |
| 3 | 0.62 | 0.47 | 0.68 | 0.55 | 3 | 0.66 | 0.36 | 0.75 | 0.42 |
| 4 | 0.65 | 0.5 | 0.6 | 0.47 | 4 | 0.83 | 0.67 | 0.7 | 0.56 |
| 5 | 0.67 | 0.53 | 0.65 | 0.44 | 5 | 0.72 | 0.67 | 0.73 | 0.56 |
| 31 | 1.33 | 1.03 | 0.99 | 0.89 | 31 | 0.98 | 0.75 | 1.03 | 0.84 |
| 32 | 1.29 | 0.73 | 1.2 | 0.81 | 32 | 1.19 | 0.79 | 1.05 | 0.96 |
| 33 | 1.36 | 0.87 | 1.18 | 0.45 | 33 | 1.06 | 0.76 | 0.99 | 0.87 |
| 34 | 0.97 | 0.72 | 1.16 | 0.66 | 34 | 1.05 | 0.79 | 1.19 | 0.75 |
| 35 | 1.13 | 0.61 | 0.9 | 0.57 | 35 | 0.96 | 0.79 | 1.19 | 0.75 |
| 61 | 1.5 | 1.08 | 1.64 | 1.19 | 61 | 1.05 | 0.84 | 1.13 | 0.88 |
| 62 | 1.52 | 1.32 | 1.88 | 1.4 | 62 | 1.34 | 1.14 | 1.21 | 1.1 |
| 63 | 1.9 | 1.13 | 1.82 | 1.33 | 63 | 1.15 | 1.08 | 1.29 | 0.9 |
| 64 | 1.4 | 0.86 | 1.75 | 1.01 | 64 | 1.11 | 1.05 | 1.06 | 0.98 |
| 65 | 1.58 | 1.3 | 1.55 | 1.27 | 65 | 1.1 | 0.9 | 0.98 | 0.87 |
| 91 | 1.52 | 0.8 | 1.5 | 0.84 | 91 | 0.93 | 0.67 | 0.96 | 0.73 |
| 92 | 1.5 | 0.92 | 1.78 | 0.73 | 92 | 0.89 | 0.82 | 1.01 | 0.81 |
| 93 | 1.44 | 0.94 | 1.51 | 0.94 | 93 | 0.85 | 0.78 | 1 | 0.76 |
| 94 | 1.42 | 1.13 | 1.38 | 1.16 | 94 | 0.79 | 0.68 | 0.99 | 0.72 |
| 95 | 1.28 | 0.84 | 1.51 | 0.67 | 95 | 0.79 | 0.74 | 0.97 | 0.65 |
| 114 | 0.35 | 0.38 | 0.58 | 0.31 | 112 | 0.71 | 0.61 | 0.8 | 0.65 |
| 115 | 0.55 | 0.31 | 0.36 | 0.36 | 113 | 0.65 | 0.58 | 0.71 | 0.63 |
| 116 | 0.6 | 0.47 | 0.48 | 0.34 | 114 | 0.78 | 0.62 | 0.75 | 0.52 |
| 117 | 0.85 | 0.45 | 0.79 | 0.58 | 115 | 0.7 | 0.66 | 0.6 | 0.49 |
| 118 | 0.99 | 0.66 | 0.84 | 0.45 | 116 | 0.7 | 0.61 | 0.67 | 0.58 |